Long-range forces between polar alkali-metal diatoms aligned by external electric fields

Jason N. Byrd, John A. Montgomery, Jr., and Robin Côté
Department of Physics, University of Connecticut, Storrs, Connecticut 06269, USA
(Received 15 July 2012; published 25 September 2012)

Long-range electrostatic, induction, and dispersion coefficients including terms of order R^{-8} have been calculated by the sum over states method using time-dependent density-functional theory. We also computed electrostatic moments and static polarizabilities of the individual diatoms up to the octopole order using coupled-cluster and density-functional theory. The laboratory-frame transformed electrostatic moments and van der Waals coefficients corresponding to the alignment of the diatomic molecules were found. We use this transformation to obtain the coupling induced by an external dc electric field and present values for all XY combinations of like polar alkali-metal diatomic molecules with atoms from Li to Cs. Analytic solutions to the dressed-state laboratory-frame electrostatic moments and long-range intermolecular potentials are also given for the dc low-field limit.

DOI: 10.1103/PhysRevA.86.032711 PACS number(s): 34.20.Gj, 33.15.Kr, 31.15.ee, 31.15.ap

I. INTRODUCTION

Advances in the formation of ultracold absolute ground-state polar alkali-metal diatoms [1,2] open up avenues into many branches of the physical sciences. For chemical physics, applications of polar diatoms range from precision spectroscopy [3,4] to the study [5–8] and control [9] of cold chemical reactions. Other areas of physics benefit from the use of polar molecules, such as condensed-matter physics [10], with the search for novel quantum gases [11] and phases [12]. Furthermore, dipolar gases have been the subject of much interest from the quantum information community [13–15], and ideas of atom optics (e.g., using evanescent wave mirrors [16]) have been generalized to polar molecules [17,18]. The recent achievements in molecular alignment and control [19,20] may also allow us to take advantage of the unique properties and possible control provided by ultracold polar molecules. In addition, there is growing interest in reactions of alkali-metal diatoms to form tetramer structures [21–23] with reasonable dipole moments and rich molecular structures, which could offer good candidates for quantum computing with dipoles [24]. In each of these applications it is crucial to accurately describe the intermolecular interactions, themselves dominated by their long-range behavior [25] at the low temperatures found in these systems. Because of the weakness of the long-range intermolecular forces compared to the chemical bond and the range of nuclear coordinates and phase space involved, it is advantageous to consider alternative methods of modeling the intermolecular potential other than *ab initio* quantum chemical calculations.

A standard approach to describing the long-range interaction potential between two molecules, in the limit that the wave function overlap between the molecules is negligible, is to expand the interaction energy into three distinct components,

$$E_{\rm int} = E_{\rm el} + E_{\rm ind} + E_{\rm disp}. \tag{1}$$

Here $E_{\rm el}$, $E_{\rm ind}$, and $E_{\rm disp}$ are the permanent electrostatic, induction (permanent-induced electrostatic), and dispersion energies. Each of these terms can be perturbatively expanded in an asymptotic van der Waals series,

$$E_{\rm LR} = \sum_n C_n R^{-n}. \tag{2}$$

The coefficients C_n are, in general, angular dependent and can be computed in several ways. In this work we expand the intermolecular electronic interaction operator in a multipole expansion [26] and then use first- and second-order perturbation theory to calculate the van der Waals coefficients. Several papers have discussed the isotropic R^{-6} interactions of homonuclear alkali-metal diatoms using both the London approximation [27] and time-dependent density-functional theory (TD-DFT) [28,29]. The isotropic and anisotropic contributions have been investigated using configuration interaction [30] and TD-DFT [31] to compute van der Waals coefficients through R^{-8}. However, systematic research on the heteronuclear alkali-metal diatoms is limited to the R^{-6} isotropic van der Waals coefficients for the LiX (X = Na, K, Rb, Cs) species [8]. To date, the only heteronuclear anisotropic van der Waals coefficients available in the literature are for KRb and RbCs [32] and are limited to R^{-6} dispersion forces. In this paper we present a systematic study of the isotropic and anisotropic van der Waals interactions through order R^{-8} of the heteronuclear alkali-metal rigid-rotor diatoms in their absolute ground state as a continuation of our work on the homonuclear species [31]. Also included is the transformation of the long-range interaction potential from the molecule-fixed (MF) frame to the laboratory-fixed (LF) frame for use in molecular alignment computations. After a brief description of dressed-state diatomic molecules in Sec. II, we review the sum-over-states method of calculating van der Waals coefficients in Sec. III. In Sec. IV the transformation to and matrix elements of the laboratory-fixed frame van der Waals interaction potential are described. Analytic expressions of the low-field field-coupled electrostatic moments and van der Waals coefficients are also provided. The *ab initio* methodology is outlined in Sec. V, and we conclude in Sec. VI with a discussion of our numerical results.

II. DRESSED-STATE DIATOMIC MOLECULES

The orientation and alignment [$\langle\cos\theta\rangle$ and $\langle\cos^2\theta\rangle$, respectively [37], as illustrated in Fig. 1(a)] of polar molecules can be

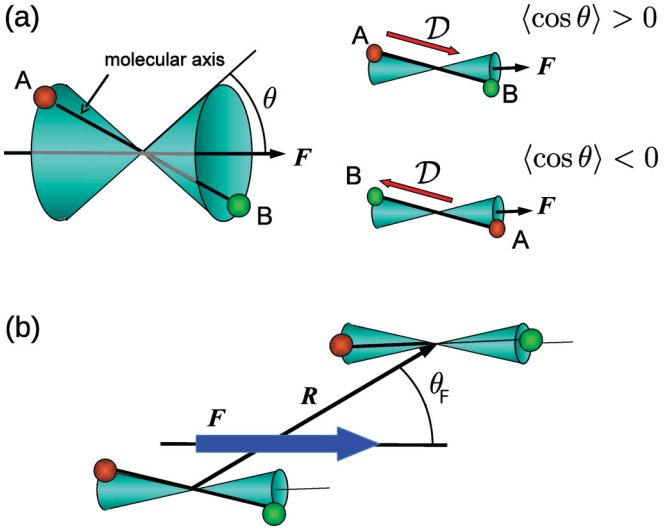

FIG. 1. (Color online) (a) Schematic representation of an aligned diatomic molecule. Classically, the molecule precesses on a cone of angle θ about the electric field $\mathbf{F}$, with $\langle\cos\theta\rangle$ describing the average orientation of the molecule: its dipole moment $\mathcal{D}$ points towards $\mathbf{F}$ for $\langle\cos\theta\rangle > 0$ and in the opposite direction for $\langle\cos\theta\rangle < 0$. The alignment, $\langle\cos^2\theta\rangle$, describes the tightness of the rotational cone. (b) Lab-fixed frame molecular interaction geometry in the presence of an external field, where θ_F is the angle between the field and the vector $\mathbf{R}$ joining the two molecules.

achieved through several mechanisms, the most direct of which is the coupling of rotational states by a polarizing external dc electric field $\mathbf{F}$. Increasing the strength F of the external electric field increases the number of rotational states coupled, thus tightening the orientation of the molecule in a cone of angle θ about the orientation of the field. To account for this rotational coupling adiabatically, we expand the dressed-state rotational wave function of the molecule as a superposition of field-free symmetric top states,

$$|\tilde{J}\tilde{M}\Omega\rangle = \sum_{J,M} a_M^J |JM\Omega\rangle, \tag{3}$$

where the symmetric top states are given in terms of Wigner rotation matrices $D^J_{-M-\Omega}(\alpha,\beta,\gamma)$ [38]:

$$|JM\Omega\rangle = (-1)^{M-\Omega}\left(\frac{2J+1}{8\pi^2}\right) D^J_{-M-\Omega}(\alpha,\beta,\gamma), \tag{4}$$

where (α,β,γ) are the Euler angles of the molecule and J is the total angular momentum quantum number with projections M in the laboratory frame and Ω onto the molecular axis. The expansion coefficients a_M^J dictate the levels of mixing between the different rotational states and can be solved for by diagonalizing $\langle\tilde{J}'\tilde{M}'\Omega'|H|\tilde{J}\tilde{M}\Omega\rangle$. Here H is the symmetric top and dipole-field Hamiltonian

$$H = B\left(\mathbf{J}^2 + J_z^2\right) - \mathcal{D}F\cos\theta, \tag{5}$$

where $\mathbf{J}$ is the angular momentum operator, J_z is the angular momentum projection on the z axis, B is the molecular rotational constant, $\mathcal{D}$ is the dipole moment of the molecule, and θ is the angle between the external electric field of magnitude F and the molecular axis. The coefficients $a_M^J(F)$ then depend on the strength F of the field. While theoretically simple, this process can become experimentally challenging for molecules with small dipole moments or rotational constants due to the large external fields required for strong alignment.

An alternative to simply increasing the static field magnitude is to add a separate polarizing laser field [39] that directly couples the rotational states of the molecule. However, to achieve both alignment and orientation control, time-dependent nonadiabatic effects are introduced into the dressed-state wave function [20]. For the purposes of this work the investigation and inclusion of these nonadiabatic effects are unimportant as only the final dressed state is of interest. As such we present our alignment in terms of an applied external static field and, where practical, the number of strongly coupled rotational states.

III. ANISOTROPIC LONG-RANGE INTERACTIONS

Given a linear molecule in the Born-Oppenheimer approximation (no nuclear motion), at any given configuration the orientation of each molecule can be described by the vector $\hat{r}_i = (\theta_i,\phi_i)$ with the relative position between the molecular center of mass defined as $\mathbf{R} = (R,\theta,\phi)$. Here θ_i is the projection angle of $\hat{r}_i$ on $\mathbf{R}$, ϕ_i is the projection angle of $\hat{r}_i$ on the x axis, and (R,θ,ϕ) are the spherical vector components of $\mathbf{R}$. Due to the rotational invariance of the interaction energy between two molecules, it can be separated into a series of radial and angular basis functions:

$$E_{\rm int}(\hat{r}_1,\hat{r}_2,\mathbf{R}) = \sum_{L_1,L_2,L} E_{L_1L_2L}(R) A_{L_1L_2L}(\hat{r}_1,\hat{r}_2,\hat{R}). \tag{6}$$

Here $E_{L_1L_2L}(R)$ are purely radial functions for a rigid rotor and $A_{L_1L_2L}(\hat{r}_1,\hat{r}_2,\hat{R})$ is an angular basis which, when $\mathbf{R}$ is oriented along the z axis, can be expressed as [40]

$$A_{L_1L_2L}(\hat{r}_1,\hat{r}_2,\hat{R}) = \sum_{M=0}^{\min(L_1,L_2)} \eta^M_{L_1L_2L} P^M_{L_1}(\cos\theta_1) P^M_{L_2}(\cos\theta_2) \times \cos[M(\phi_1-\phi_2)], \tag{7}$$

where

$$\eta^M_{L_1L_2L} = (-1)^M(2-\delta_{M,0})(L_1M;L_2-M|L0) \times\left[\frac{(L_1-M)!(L_2-M)!}{(L_1+M)!(L_2+M)!}\right]^{1/2}, \tag{8}$$

$(L_1M;L_2-M|L0)$ is a Clebsch-Gordan coefficient, and $P^M_L(\cos\theta)$ is an associated Legendre polynomial. The radial functions $E_{L_1L_2L}(R)$ can be evaluated using first- and second-order perturbation theory by expanding in terms of the electronic multipole operators $Q_{\ell m} = \sum_i z_i r_i^\ell C_{\ell m}(\hat{r}_i)$, where the sum is over each charge i, z_i is the charge at each ith center, r_i^ℓ is the distance from each ith charge to the center of mass, and $C_{\ell m}(\hat{r}_i)$ is a Racah spherical harmonic [38].

Following the standard approach [26,31,41], the first- and second-order interaction energy for two linear molecules can be expressed as

$$E_{\rm int}(R,\theta_1,\theta_2,\phi) = \sum_{n,L_1,L_2,M} \frac{\left(W^{(1)}_{nL_1L_2M} - W^{(2)}_{nL_1L_2M}\right)}{R^n} \times P^M_{L_1}(\cos\theta_1) P^M_{L_2}(\cos\theta_2)\cos[M\phi], \tag{9}$$

where $\phi \equiv \phi_1 - \phi_2$ and

$$W^{(1)}_{nL_1L_2M} = (-1)^{L_1+M}(2-\delta_{M,0})\frac{(L_1+L_2)!}{(L_1+M)!(L_2+M)!} \times \langle 0_1|Q_{L_10}|0_1\rangle\langle 0_2|Q_{L_20}|0_2\rangle \quad (10)$$

is the first-order electrostatic contribution, where $|0_i\rangle$ is the electronic ground state of molecule i. In Eq. (9),

$$W^{(2)}_{nL_1L_2M} = W^{(2,\mathbf{DIS})}_{nL_1L_2M} + W^{(2,\mathbf{IND})}_{nL_1L_2M} \quad (11)$$

contains the second-order contributions from dispersion,

$$W^{(2,\mathbf{DIS})}_{nL_1L_2M}(R) = \sum_{\substack{\ell_1,\ell_1'\\ \ell_2,\ell_2'}} \zeta^{\ell_1\ell_1';\ell_2\ell_2'}_{L_1L_2M}\delta_{\ell_1+\ell_1'+\ell_2+\ell_2'+2,n} \times \sum_{\substack{k_1\neq 0\\ k_2\neq 0}} \frac{T^{0_1k_1}_{\ell_1\ell_1'L_1}T^{0_2k_2}_{\ell_2\ell_2'L_2}}{\epsilon_{k_1}-\epsilon_{0_1}+\epsilon_{k_2}-\epsilon_{0_2}}, \quad (12)$$

and induction,

$$W^{(2,\mathbf{IND})}_{nL_1L_2M}(R) = \sum_{\substack{\ell_1,\ell_1'\\ \ell_2,\ell_2'}} \zeta^{\ell_1\ell_1';\ell_2\ell_2'}_{L_1L_2M}\delta_{\ell_1+\ell_1'+\ell_2+\ell_2'+2,n} \times \left(T^{0_1k_1}_{\ell_1\ell_1'L_1}\sum_{k_2\neq 0}\frac{T^{0_2k_2}_{\ell_2\ell_2'L_2}}{\epsilon_{k_2}-\epsilon_{0_2}} + (1\rightleftharpoons 2)\right). \quad (13)$$

The scalar coupling coefficient $\zeta^{\ell_1\ell_1';\ell_2\ell_2'}_{L_1L_2M}$ is given [40] as

$$\zeta^{\ell_1\ell_1';\ell_2\ell_2'}_{L_1L_2M} = (-1)^{\ell_2+\ell_2'}[(2L_1+1)!(2L_2+1)!]^{1/2} \times \left[\frac{(2\ell_1+2\ell_2+1)!(2\ell_1'+2\ell_2'+1)!}{(2\ell_1)!(2\ell_1')!(2\ell_2)!(2\ell_2')!}\right]^{1/2} \times \sum_L \eta^M_{L_1,L_2,L}(\ell_1+\ell_20;\ell_1'+\ell_2'0|L0) \times \begin{Bmatrix} \ell_1 & \ell_1' & L_1\\ \ell_2 & \ell_2' & L_2\\ \ell_1+\ell_2 & \ell_1'+\ell_2' & L\end{Bmatrix}, \quad (14)$$

the symbol between curly brackets being a Wigner $9j$ symbol [38], and $T^{0_ik_i}_{\ell_i\ell_i'L_i}$ is the coupled monomer multipole transition moment, defined as

$$T^{0_ik_i}_{\ell_i\ell_i'L_i} = \sum_m \langle 0_i|Q_{\ell_im}|k_i\rangle\langle k_i|Q_{\ell_i'-m}|0_i\rangle(\ell_im;\ell_i'-m|L_i0), \quad (15)$$

where the indices k_i go over ground and excited states of the ith molecule's electronic wave function $|k_i\rangle$ [42]. It is convenient, when discussing molecular properties, to work with the uncoupled dynamic multipole polarizability:

$$\alpha_{\ell\ell'm}(\omega) = \sum_{k\neq 0}\frac{(\epsilon_k-\epsilon_0)\langle 0_i|Q_{\ell m}|k_i\rangle\langle k_i|Q_{\ell'-m}|0_i\rangle}{(\epsilon_k-\epsilon_0)^2-\omega^2}. \quad (16)$$

The zero-frequency limit of Eq. (16) represents the static multipole polarizability.

IV. DRESSED-STATE VAN DER WAALS INTERACTION

A. General expressions

To consider the interactions between rigid-rotor linear molecules dressed by an external electric field it is necessary to first transform the van der Waals interaction energy from the MF to the LF. The laboratory-fixed frame van der Waals interaction can be generally expressed by referring to Eq. (6) and removing the constraint on Eq. (7) which specified that **R** is aligned to the z axis. The angular basis can then generally be expressed [41] as

$$A_{L_1L_2L}(\hat{R},\hat{r}_1,\hat{r}_2) = \sum_{m_{L_1},m_{L_2},m_L}\begin{pmatrix} L_1 & L_2 & L\\ m_{L_1} & m_{L_2} & m_L\end{pmatrix} \times Y_{L_1m_{L_1}}(\hat{r}_1)Y_{L_2m_{L_2}}(\hat{r}_2)Y_{Lm_L}(\hat{R}), \quad (17)$$

where $Y_{\ell m_\ell}(\hat{r})$ is a spherical harmonic and (:::) is a Wigner $3j$ symbol [38]. Because of the change in angular basis, it is necessary to recouple the radial $W^{(1,2)}_{nL_1L_2M}$ functions. This can be done readily by integrating Eq. (9) over the angular phase space:

$$E^{\mathrm{LF}}_{L_1L_2L}(R) = \frac{1}{\sqrt{8\pi}}\int_0^{2\pi}d\phi\int_0^{\pi}d\theta_1\int_0^{\pi}d\theta_2\sin(\theta_1)\sin(\theta_2) \times A'_{L_1L_2L}(\theta_1,\theta_2,\phi)E^{\mathrm{MF}}_{\mathrm{int}}(R,\theta_1,\theta_2,\phi), \quad (18)$$

where $A'_{L_1,L_2,L}(\theta_1,\theta_2,\phi)$ is Eq. (17) projected onto the molecule-fixed frame and is given by Ref. [43]

$$A'_{L_1L_2L}(\theta_1,\theta_2,\phi) = \left(\frac{2L+1}{2\pi}\right)^{1/2}\sum_{m=0}^{\min(L_1,L_2)}(-1)^m(2-\delta_{m,0}) \times \begin{pmatrix} L_1 & L_2 & L\\ m & -m & 0\end{pmatrix}\Theta_{L_1m}(\theta_1) \times \Theta_{L_2m}(\theta_2)\cos[m\phi], \quad (19)$$

where $\Theta_{lm}(\theta)$ are normalized associated Legendre polynomials. The resulting integrand has the solution

$$E^{\mathrm{LF}}_{L_1L_2L}(R) = \sum_M(-1)^M\begin{pmatrix} L_1 & L_2 & L\\ M & -M & 0\end{pmatrix} \times \left(\frac{(L_1+M)!(L_2+M)!}{(L_1-M)!(L_2-M)!}\right)^{1/2} \times \left(\frac{2L+1}{(2L_1+1)(2L_2+1)}\right)^{1/2} \times \sum_n\frac{(W^{(1)}_{nL_1L_2M}-W^{(2)}_{nL_1L_2M})}{R^n}. \quad (20)$$

The adiabatic dressed-state basis for two molecules at large separation is given in terms of the product of each molecule's dressed rotational wave functions:

$$|\phi\rangle = |\tilde{J}_1\tilde{M}_1\Omega_1\rangle\otimes|\tilde{J}_2\tilde{M}_2\Omega_2\rangle. \quad (21)$$

The dressed-state (DS) van der Waals interaction $E^{\mathrm{DS}}_{\mathrm{int}}(\mathbf{R})$ is calculated from the matrix elements of Eq. (20) in the

dressed-state basis,

$$E_{\rm int}^{\rm DS}(\mathbf{R},F) = \langle \tilde{J}_2' \tilde{M}_2' \Omega_2' | \langle \tilde{J}_1' \tilde{M}_1' \Omega_1' | E_{\rm int}^{\rm LF}(\hat{r}_1,\hat{r}_2,\mathbf{R}) | \tilde{J}_1 \tilde{M}_1 \Omega_1 \rangle | \tilde{J}_2 \tilde{M}_2 \Omega_2 \rangle = \sqrt{4\pi} \sum_{\substack{J_1,M_1\\J_1',M_1'}} \sum_{\substack{J_2,M_2\\J_2',M_2'}} \sum_{\substack{L_1,m_{L_1}\\L_2,m_{L_2}}} \delta_{\Omega_1,\Omega_1'} \delta_{\Omega_2,\Omega_2'}$$
$$\times (-1)^{M_1-\Omega_1+m_{L_1}} (-1)^{M_2-\Omega_2+m_{L_2}} \rho_{M_1'M_1}^{J_1'J_1}(F) \rho_{M_2'M_2}^{J_2'J_2}(F) [(2J_1+1)(2J_1'+1)(2J_2+1)(2J_2'+1)(2L_1+1)$$
$$\times (2L_2+1)]^{1/2} \begin{pmatrix} J_1' & L_1 & J_1 \\ M_1' & m_{L_1} & -M_1 \end{pmatrix} \begin{pmatrix} J_1' & L_1 & J_1 \\ \Omega_1 & 0 & -\Omega_1 \end{pmatrix} \begin{pmatrix} J_2' & L_2 & J_2 \\ M_2' & m_{L_2} & -M_2 \end{pmatrix} \begin{pmatrix} J_2' & L_2 & J_2 \\ \Omega_2 & 0 & -\Omega_2 \end{pmatrix}$$
$$\times \sum_{L,m_L} \begin{pmatrix} L_1 & L_2 & L \\ m_{L_1} & m_{L_2} & m_L \end{pmatrix} Y_{Lm_L}(\hat{R}) E_{L_1L_2L}^{\rm LF}(R), \tag{22}$$

where

$$\rho_{M_i'M_i}^{J_i'J_i}(F) = a_{M_i'}^{J_i'}(F) a_{M_i}^{J_i}(F) \tag{23}$$

is the coupled rotational state density of molecule i and $Y_{Lm}(\hat{r})$ is a spherical harmonic [38]. In addition to the transformation of the van der Waals interaction energy as given by Eq. (22), it is useful to have the dressed static moment $\langle Q_{\ell 0}^{DS} \rangle$ of a given molecule. For molecule i, this is readily obtained to be

$$\left\langle Q_{\ell 0}^{DS} \right\rangle = \langle \tilde{J}_i' \tilde{M}_i' \Omega_i' | \langle 0_i | Q_{\ell 0} | 0_i \rangle | \tilde{J}_i \tilde{M}_i \Omega_i \rangle (F) = \sum_{\substack{J_i,J_i'\\M_i}} \delta_{\Omega_i,\Omega_i'} \delta_{M_i,M_i'} \rho_{M_iM_i}^{J_i'J_i}(F) [(2J_i+1)(2J_i'+1)]^{1/2}$$
$$\times (-1)^{M_i-\Omega_i} \begin{pmatrix} J_i' & \ell & J_i \\ M_i' & 0 & -M_i \end{pmatrix} \begin{pmatrix} J_i' & \ell & J_i \\ \Omega_i & 0 & -\Omega_i \end{pmatrix} \langle Q_{\ell 0} \rangle. \tag{24}$$

B. Low-field solution

In the low-field limit, coupling between rotational states can be limited to just two states, allowing Eq. (5) to be solved analytically (note that $\Omega \equiv 0$ and $M = 0$, as discussed below in Sec. VI). From this it is possible to obtain general expressions for the expectation value of the static and alignment moments as a function of the applied field. Transforming to the unitless field parameter $\xi = \xi_0 F$, with $\xi_0 \equiv \mathcal{D}/2B$, the low-field limit is defined by $\xi \leqslant 1$. With this approximation, the dressed-state dipole and quadrupole moments can be shown to be

$$\left\langle Q_{10}^{\rm DS} \right\rangle (\xi) = \langle Q_{10} \rangle \frac{6\xi + 2\xi^3}{8(1+\xi^2)} \tag{25}$$

and

$$\left\langle Q_{20}^{\rm DS} \right\rangle (\xi) = \langle Q_{20} \rangle \frac{2\xi^2}{15(1+\xi^2)}, \tag{26}$$

respectively, while the octopole moment has no two-state contribution by symmetry. The orientation moment $\langle \cos\theta \rangle$ is given trivially by

$$\langle \cos\theta \rangle (\xi) = \left\langle Q_{10}^{\rm DS} \right\rangle (\xi) / \langle Q_{10} \rangle, \tag{27}$$

while alignment $\langle \cos^2\theta \rangle$ can be calculated by noting that $\cos^2\theta = \frac{1}{3}[1 + 2C_{1,0}(\theta)]$ [where $C_{\ell,m}(\hat{r}_i)$ is a Racah spherical harmonic], providing the expression

$$\langle \cos^2\theta \rangle (\xi) = \frac{15 + 19\xi^2}{45(1+\xi^2)}. \tag{28}$$

So long as the number of coupled states is dominated by the first two states and $\xi \leqslant 1$, these approximate formulas are accurate to a few percent. We have evaluated ξ_0 for all the heteronuclear alkali-metal diatoms from the spectroscopic data in given in Table I, and we present the results in Table II. It is also possible to evaluate Eqs. (22) and (23) using the two-state low-field approximation. Following the prescribed method discussed above, the low-field dressed-state van der Waals potential can be written to leading order as

$$E_{\rm 2st}^{\rm DS}(\mathbf{R},\xi) \simeq \frac{\tilde{W}_{320}^{(1)}(\theta_F,\xi)}{R^3} + \frac{\tilde{W}_{540}^{(1)}(\theta_F,\xi)}{R^5} - \frac{W_{6000}^{(2)}}{R^6} - \frac{W_{8000}^{(2)}}{R^8}. \tag{29}$$

Here θ_F is the angle between the intermolecular vector $\mathbf{R}$ and the field vector, as illustrated in Fig. 1(b). The dipole-dipole and quadrupole-quadrupole contributions are (up to order ξ^5)

$$\tilde{W}_{320}^{(1)}(\theta_F,\xi) = \langle Q_{10} \rangle^2 \frac{3\sqrt{3}\xi + 6\xi^2 + 4\sqrt{3}\xi^3 + 4\xi^4}{27(1+\xi^2)^2} \times (1 - 3\cos^2\theta_F) \tag{30}$$

and

$$\tilde{W}_{540}^{(1)}(\theta_F,\xi) = \langle Q_{20} \rangle^2 \frac{\xi^4}{75(1+\xi^2)^2} \times (3 - 30\cos^2\theta_F + 35\cos^4\theta_F), \tag{31}$$

respectively (note that there is no dipole-octopole contribution in the two-state approximation), while $W_{n000}^{(2)}$ is the isotropic dispersion + induction coefficient (see Tables IV and V). The anisotropic terms contribute less than a percent to the interaction energy and can be safely neglected.

TABLE I. Center-of-mass multipole electrostatic moments $\langle Q_{\ell 0}\rangle$ ($\ell = 1,2,3$ corresponds to dipole, quadrupole, and octopole moments, respectively) of all the ground-state heteronuclear alkali-metal diatoms through cesium evaluated at the equilibrium bond length r_e. The variable R_q denotes the distance where the R^{-5} electrostatic term overcomes the dipole-dipole R^{-3} contribution. All values are presented in atomic units.

System	Method	r_e[a]	$\langle Q_{10}\rangle$	$\langle Q_{20}\rangle$	$\langle Q_{30}\rangle$	R_q
LiNa	CCSD(T)[b]	5.45	0.20	10.07	−47.33	95
	VCI[c]	5.43	0.22			
	CCSDT[d]	5.45	0.21			
LiK	CCSD(T)[b]	6.27	1.39	6.07	−59.99	15
	VCI[c]	6.21	1.39			
	CCSDT[d]	6.27	1.38			
LiRb	CCSD(T)[b]	6.50	1.63	2.76	−62.41	13
	VCI[c]	6.48	1.63			
	CCSDT[d]	6.50	1.59			
LiCs	CCSD(T)[b]	6.93	2.15	−2.29	−49.88	10
	VCI[c]	6.82	2.17			
	CCSDT[d]	6.93	2.11			
NaK	CCSD(T)[b]	6.61	1.12	10.56	−26.54	19
	CCSD(T)[e]	6.592	1.156	10.60		
	VCI[c]	6.49	1.09			
NaRb	CCSD(T)[b]	6.88	1.35	6.94	−56.00	16
	VCI[c]	6.84	1.30			
NaCs	CCSD(T)[b]	7.27	1.85	2.49	−60.45	12
	VCI[c]	7.20	1.83			
KRb	CCSD(T)[b]	7.69	0.25	15.14	−69.09	109
	VCI[c]	7.64	0.23			
	rel[f]	7.7	0.30			
KCs	CCSD(T)[b]	8.10	0.75	13.00	−105.70	38
	VCI[c]	8.02	0.76			
RbCs	CCSD(T)[b]	8.37	0.49	15.88	−50.28	60
	VCI[c]	8.30	0.40			

[a]The r_e values are taken from experimental results where available; see Deiglmayr *et al.* [33] and references therein.
[b]This work.
[c]Reference [34].
[d]Reference [8].
[e]Reference [27].
[f]Reference [35] performed a four-component Dirac-Fock valence bond calculation in calculating the dipole moment.

V. ELECTRONIC STRUCTURE CALCULATIONS

The *ab initio* calculation of van der Waals coefficients, and more generally multipole polarizabilities, requires special care in both the basis set and level of theory used [44–46]. Electrostatic moments similarly require careful consideration of the theoretical method, though the basis-set dependence is less severe [47]. For all calculations in this work we use the Karlsruhe def2-QZVPP [48] basis set augmented with two additional even-tempered diffuse $spdf$ functions designed to accurately describe higher-order static polarizabilities [31]. The Karlsruhe def2 basis sets are available for nearly the entire periodic table and are known for both their robustness and good cost-to-performance ratio in large molecular Hartree-Fock and density-functional theory calculations. As such, they remain attractive for use in calculations that involve many different atoms across the periodic table.

TABLE II. Tabulated values of the field strength coefficient $\xi_0 = \mathcal{D}/2B$ using the spectroscopic and electrostatic constants from Table I. All units are in $\mathrm{cm}^2/\mathrm{kV}$.

	^{23}Na	^{39}K	^{95}Rb	^{133}Cs
^{7}Li	0.0114	0.116	0.159	0.246
^{23}Na		0.253	0.413	0.684
^{39}K			0.141	0.529
^{95}Rb				0.635

As has been demonstrated previously, the use of time-dependent density-functional theory [49,50] is a cost-effective and accurate way to calculate multipole transition moments and excitation energies for diatomic molecules. We chose to limit our calculations in this work to only include the PBE0 functional for simplicity; however, for various cases it was observed that the B3PW91 functional also provides consistent results. The electrostatic moments were calculated using coupled-cluster theory including all singles, doubles, and perturbative triples [CCSD(T)] [51] using a two-step finite-field method (with field spacings of 10^{-6} a.u.). Core-valence and core-core correlation energy was accounted for by including the inner valence s and p electrons in the CCSD(T) calculations, while for the TD-DFT computations all electrons not replaced by an effective core potential (ECP) are implicitly correlated. All TD-DFT calculations were done using a locally modified version of the GAMESS [52,53] suite of programs; the CCSD(T) finite-field calculations were done using the MOLPRO [54] quantum chemistry program package. For further details on the methodology used in evaluating the transition dipole moments and excitation energy we refer to our previous paper on homonuclear alkali-metal diatomic molecules [31].

VI. COMPUTATIONAL RESULTS AND DISCUSSION

The leading-order term of the long-range expansion Eq. (9), and thus the longest-ranged interaction in the series, involves products of the electrostatic moments of each monomer, and for dipolar molecules, it is the dipole-dipole R^{-3} term. The dipole-dipole scattering [55] and applications of dipole-dipole interactions [14] are well studied in the literature; however, higher-order terms can be necessary for accurately describing intermediate intermolecular distances [31] and are often neglected if only for a lack of available data. Inclusion of just the quadrupole-quadrupole interaction to a dipole-dipole model can introduce significant changes in the form of potential energy barriers for collinear geometries ($\theta_1 = \theta_2 = \phi = 0$) at long range [56]. It is possible to estimate whether the inclusion of higher-order electrostatic terms could lead to a barrier by introducing the outer zero-energy turning point R_q, which occurs when the R^{-5} repulsion overcomes the attractive R^{-3} dipole-dipole force. Keeping only the two leading terms in Eq. (9) and setting

$$E_{\mathrm{int}}(R_q,0,0,0) = -\frac{\langle Q_{10}\rangle^2}{R_q^3} + \frac{3\langle Q_{20}\rangle^2 - 4\langle Q_{10}\rangle\langle Q_{30}\rangle}{R_q^5} = 0, \tag{32}$$

we obtain

$$R_q = \frac{\sqrt{3\langle Q_{20}\rangle^2 - 4\langle Q_{10}\rangle\langle Q_{30}\rangle}}{\langle Q_{10}\rangle}. \quad (33)$$

When this outer turning point is sufficiently long range ($R_q \gtrsim 20$ a.u.), the introduction of these higher-order terms can be important and lead to long-range barriers [56] and thus should be examined in further detail [57]. As such, we have calculated the *ab initio* electrostatic dipole, quadrupole, and octopole moments (higher-order moments do not contribute up to R^{-5} in the long-range expansion; see Sec. V for details on the methodology used). In Table I we present our calculated static moments, the outer turning point R_q for each system, and various dipole and quadrupole moments found in the literature. Our computed static dipole moments agree closely with both the valence full-configuration interaction results of Aymar and Dulieu [34] and González-Férez *et al.* [58] across all the molecules investigated, and the CCSDT (CCSD with all triples) results of Quéméner *et al.* [8] for the highly polar LiX (X = Na, K, Rb, Cs) species. Other than the CCSD(T) quadrupole moment of Zemke *et al.* [27] (with which we compare well), little to no published quadrupole values exist for the heteronuclear alkali-metal diatoms. It has been demonstrated for the homonuclear alkali-metal diatoms that the finite-field CCSD(T) higher-order static moments compare well with other methods [31,47]; similar accuracy is anticipated for the heteronuclear species.

Dispersion and induction contributions to the van der Waals series are proportional to products of the dipole, quadrupole, and octopole polarizabilities. As such, we have calculated and presented in Table III the dipole and quadrupole static polarizabilities with comparisons to some of the existing literature (octopole static polarizabilities are not listed but are available upon request). As discussed previously [31], the n-aug-def2-QZVPP basis sets are well converged for

TABLE III. Multipole static polarizabilities $\alpha_{\ell\ell' m}$ and isotropic van der Waals dispersion coefficients $W_{n000}^{(2,\mathrm{DIS})}$ up to order $n = 8$ of all the ground-state alkali-metal diatoms through cesium evaluated at the equilibrium bond lengths r_e listed in Table I. All values are presented in atomic units, and [n] denotes $\times 10^n$.

System	Method	α_{110}[a]	α_{111}[a]	$\bar{\alpha}$[b]	α_{220}	α_{221}	α_{222}	$W_{6000}^{(2,\mathrm{DIS})}$	$W_{8000}^{(2,\mathrm{DIS})}$
LiNa	PBE0[c]	300.0	185.5	223.7	9418.9	7035.6	3356.2	3.279[3]	4.982[5]
	VCI[d]	347.6	181.8	237.0					
	CCSDT[e]			237.8				3.673[3][f]	
LiK	PBE0[c]	455.1	261.8	326.3	24164.4	15899.8	5939.6	5.982[3]	1.378[6]
	VCI[d]	489.7	236.2	320.7					
	CCSDT[e]			324.9				6.269[3][f]	
LiRb	PBE0[c]	445.5	256.1	319.2	27815.3	18110.7	6359.2	6.193[3]	1.583[6]
	VCI[d]	524.3	246.5	339.1					
	CCSDT[e]			346.2				6.323[3][f]	
LiCs	PBE0[c]	525.2	289.1	367.8	38723.9	24996.3	7935.8	7.700[3]	2.297[6]
	VCI[d]	597.0	262.5	374.0					
	CCSDT[e]			386.7				7.712[3][f]	
NaK	PBE0[c]	472.7	280.6	344.6	16572.0	13035.0	6739.5	6.818[3]	1.268[6]
	VCI[d]	529.2	262.3	351.3					
	CCSD(T)[g]			363.8				6.493[3][h]	
NaRb	PBE0[c]	504.6	285.3	358.4	25217.0	17771.7	7547.5	7.688[3]	1.790[6]
	VCI[d]	572.0	280.3	377.5					
NaCs	PBE0[c]	587.3	323.2	411.2	37633.3	25245.7	9444.6	9.453[3]	2.641[6]
	VCI[d]	670.7	304.2	426.4					
KRb	PBE0[c]	729.6	420.9	523.8	36974.1	27588.8	13100.9	1.349[4]	3.385[6]
	VCI[d]	748.7	382.9	504.8					
KCs	PBE0[c]	836.7	468.6	591.3	56372.9	38791.7	16262.9	1.657[4]	5.038[6]
	VCI[d]	822.3	425.62	571.1					
RbCs	PBE0[c]	901.0	502.0	635.0	48325.3	36401.8	18619.8	1.884[4]	5.188[6]
	VCI[d]	904.0	492.3	602.8					

[a]Note that the parallel and perpendicular static dipole polarizabilities, $\alpha_\parallel$ and $\alpha_\perp$, correspond to $\ell\ell' m = 110$ and 111, respectively.
[b]$\bar{\alpha} = \frac{1}{3}(\alpha_\parallel + 2\alpha_\perp)$ is the average static dipole polarizability.
[c]This work.
[d]Reference [33].
[e]Reference [8].
[f]Reference [8] evaluated using CCSD and the Tang-Slater-Kirkwood formula [36].
[g]Reference [27].
[h]Reference [27] evaluated using the London formula.

computation of static polarizabilities of homonuclear alkali-metal diatoms up to octopole order, and we find the same is true for the heteronuclear species. Density-functional methods are known to provide average static polarizabilities to within 5–10% of experimental or highly correlated results [59,60]. Furthermore some variance is expected in the parallel (α_{110}) polarizability as all computations are done at the experimental (or theoretical where necessary) equilibrium bond length, and it is well known that the polarizability is sensitive to the internuclear separation in the alkali-metal diatoms [33]. It is expected that the perpendicular polarizability (α_{111}) should agree much more closely with other methods, which we find to be the case, as illustrated in Table III.

Van der Waals dispersion and induction coefficients of the heteronuclear alkali-metal diatoms are sparsely given in the literature. Currently, only a few values exist and are restricted to isotropic contributions (corresponding to $W^{2,\mathrm{DIS}}_{6000}$). The only systematically calculations are for the LiX species [8]. In Table III we note the reasonable agreement between our reported TD-DFT isotropic $C_6 = W^{2,\mathrm{DIS}}_{6000}$ dispersion coefficients and the Tang-Slater-Kirkwood [36] values from Quéméner *et al*. [8] for the LiX species. Additionally Kotochigova [32] has calculated, using multireference configuration interaction theory, the isotropic and anisotropic dispersion coefficients of order R^{-6} for both KRb and RbCs. However, these values contain non-Born-Oppenheimer contributions and so are not directly comparable to our numbers; because of this we have not included these values in Table III. To determine the accuracy of the van der Waals coefficients calculated here, we have computed *ab initio* curves for LiNa + LiNa at two different molecular frame geometries using the CCSD(T)-F12a–QZVPP [explicitly correlated CCSD(T)] level of theory [61,62]. These *ab initio* curves are plotted in Fig. 2 along with the electrostatic plus isotropic dispersion approximation and the van der Waals curves of this work including all anisotropic terms through R^{-8}. As can be seen, the TD-DFT van der Waals curves agree to a few cm^{-1} with the *ab initio* results [63], while the isotropic curves fail completely in the intermediate range (it should be noted that for the collinear case of LiNa + LiNa the isotropic curves do not turn over at all and predict an infinite repulsive wall). In Tables IV and V we have listed the $W^{(1,2)}_{nL_1L_2M}$ coefficients for all of the heteronuclear alkali-metal diatoms, including all terms up through order R^{-8}.

In evaluating the field coupling and alignment of the various alkali-metal diatomic molecules, the rotational wave-function expansion is greatly simplified by making use of the initial

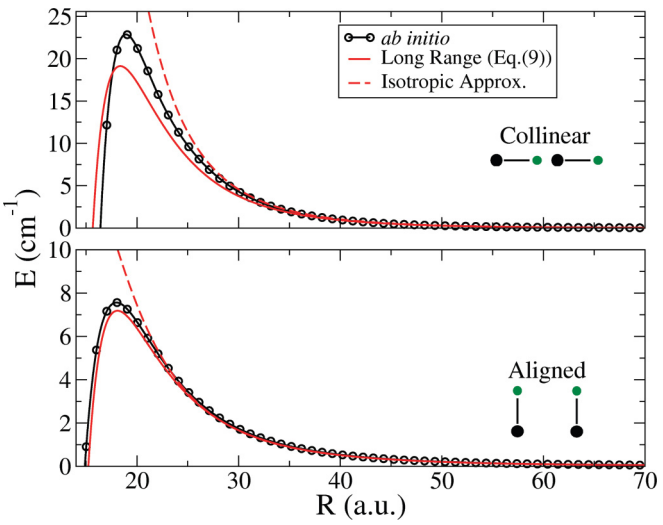

FIG. 2. (Color online) A comparison of interaction curves at various orientations for molecule-fixed-frame LiNa + LiNa (in the absence of an external electric field) at different levels of theory. The black open circles are a fully *ab initio* curve computed at the CCSD(T)-f12a–QZVPP level of theory (see text for computational details), the solid red line is the evaluation of the van der Waals expansion of Eq. (9) using TD-DFT to compute the dispersion coefficients (see Tables IV and V), and the dashed red line is the usual isotropic approximation containing angular-dependent electrostatic terms where the dispersion contribution is truncated at the isotropic C_6 coefficient.

TABLE IV. LiX (X = Na, K, Rb, Cs) calculated CCSD(T) electrostatic and TD-DFT dispersion + induction van der Waals coefficients $W^{(1,2)}_{nL_1L_2M}$ for unique combinations of L_1L_2M. All values are presented in atomic units and calculated at the equilibrium bond length r_e listed in Table I, and [n] denotes $\times 10^n$.

nL_1L_2M	LiNa	LiK	LiRb	LiCs
		Electrostatic: $W^{(1)}_{nL_1L_2M}$		
3110	−7.076[0]	−3.799[0]	−5.170[0]	−9.094[0]
3111	0.038[0]	1.900[0]	2.585[0]	4.547[0]
4210	−5.893[0]	−2.547[1]	−1.431[1]	1.324[1]
4211	1.965[0]	8.489[0]	4.771[0]	−4.412[0]
5220	6.086[2]	2.276[2]	5.284[1]	2.568[1]
5221	−1.353[2]	−5.058[1]	−1.174[1]	−5.707[0]
5222	8.453[0]	3.161[0]	0.734[0]	0.357[0]
5310	3.674[1]	3.306[2]	2.887[2]	3.942[2]
5311	−9.186[0]	−8.266[1]	−7.218[1]	−9.855[1]
		Dispersion + induction: $W^{(2)}_{nL_1L_2M}$		
6000	3.289[3]	7.243[3]	7.254[3]	1.062[4]
6200	4.036[2]	3.479[2]	4.874[2]	2.739[1]
6220	1.768[2]	1.180[3]	1.094[3]	2.567[3]
6221	−3.929[1]	−2.621[2]	−2.430[2]	−5.705[2]
6222	4.911[0]	3.277[1]	3.038[1]	7.131[1]
7100	1.075[3]	−4.898[2]	−5.906[3]	−3.740[4]
7210	1.460[2]	−7.641[3]	−8.641[3]	−3.110[4]
7211	−2.433[1]	1.273[3]	1.440[3]	5.184[3]
7300	7.411[2]	4.567[3]	1.057[3]	−9.020[3]
7320	4.259[2]	−7.013[2]	−2.682[3]	−1.687[4]
7321	−7.099[1]	1.169[2]	4.470[2]	2.812[3]
7322	5.070[0]	−8.349[0]	−3.193[1]	−2.008[2]
8000	5.586[5]	1.539[6]	1.715[6]	2.722[6]
8200	3.552[5]	1.270[6]	1.534[6]	2.793[6]
8220	9.460[4]	5.702[5]	6.695[5]	1.636[6]
8221	−1.406[4]	−8.078[4]	−9.379[4]	−2.272[5]
8222	1.234[3]	4.607[3]	4.642[3]	9.978[3]
8400	3.896[4]	4.574[4]	6.320[4]	1.371[5]
8420	2.706[4]	7.284[4]	8.377[4]	2.485[5]
8421	−3.666[3]	−9.822[3]	−1.124[4]	−3.320[4]
8422	2.001[2]	5.287[2]	5.965[2]	1.740[3]

TABLE V. XY (X,Y = Na, K, Rb, Cs) calculated CCSD(T) electrostatic and TD-DFT dispersion + induction van der Waals coefficients, $W^{(1,2)}_{nL_1L_2M}$, for unique combinations of L_1L_2M. All values are presented in atomic units and calculated at the equilibrium bond length r_e listed in Table I, and [n] denotes $\times 10^n$.

nL_1L_2M	NaK	NaRb	NaCs	KRb	KCs	RbCs
			Electrostatic: $W^{(1)}_{nL_1L_2M}$			
3110	−2.470[0]	−3.651[0]	−6.813[0]	−0.125[0]	−1.164[0]	−0.432[0]
3111	1.235[0]	1.826[0]	3.406[0]	0.063[0]	0.582[0]	0.216[0]
4210	−3.528[1]	−2.818[1]	−1.377[1]	−1.134[1]	−2.960[1]	−2.221[1]
4211	1.176[1]	9.393[0]	4.590[0]	3.785[0]	9.867[0]	7.403[0]
5220	6.717[2]	2.900[2]	3.710[1]	1.375[3]	1.004[3]	1.524[3]
5221	−1.493[2]	−6.444[1]	−8.245[0]	−3.056[2]	−2.231[2]	−3.386[2]
5222	9.329[0]	4.028[0]	0.515[0]	1.910[1]	1.395[1]	2.116[1]
5310	1.175[2]	7.346[1]	5.962[1]	6.909[1]	1.955[2]	1.106[1]
5311	−2.937[1]	−1.836[1]	−1.490[1]	−1.727[1]	−4.887[1]	−2.764[0]
			Dispersion + induction: $W^{(2)}_{nL_1L_2M}$			
6000	7.777[3]	8.680[3]	1.233[4]	1.354[4]	1.726[4]	1.921[4]
6200	5.519[2]	7.837[2]	3.327[2]	2.001[3]	2.375[3]	2.909[3]
6220	9.762[2]	1.223[3]	2.694[3]	1.028[3]	1.826[3]	1.857[3]
6221	−2.169[2]	−2.717[2]	−5.986[2]	−2.284[2]	−4.059[2]	−4.127[2]
6222	2.712[1]	3.397[1]	7.482[1]	2.855[1]	5.073[1]	5.159[1]
7100	1.157[4]	2.268[3]	−2.114[4]	6.069[3]	1.457[4]	1.755[4]
7210	−1.657[1]	−4.434[3]	−2.312[4]	9.929[2]	−8.871[2]	2.795[3]
7211	2.762[0]	7.391[2]	3.853[3]	−1.655[2]	1.479[2]	−4.658[2]
7300	9.136[3]	4.795[3]	−1.280[3]	4.176[3]	1.234[4]	1.231[4]
7320	4.931[3]	1.142[3]	−9.091[3]	2.772[3]	7.134[3]	8.669[3]
7321	−8.219[2]	−1.903[2]	1.515[3]	−4.621[2]	−1.189[3]	−1.445[3]
7322	5.870[1]	1.360[1]	−1.082[2]	3.300[1]	8.492[1]	1.032[2]
8000	1.444[6]	1.928[6]	3.016[6]	3.734[6]	5.391[6]	5.667[6]
8200	8.920[5]	1.503[6]	2.766[6]	2.606[6]	4.295[6]	3.923[6]
8220	3.296[5]	6.003[5]	1.466[6]	7.941[5]	1.494[6]	1.296[6]
8221	−4.768[4]	−8.470[4]	−2.042[5]	−1.162[5]	−2.138[5]	−1.878[5]
8222	3.368[3]	4.596[3]	9.349[3]	9.098[3]	1.356[4]	1.351[4]
8400	6.476[4]	6.275[4]	1.107[5]	2.931[5]	3.258[5]	4.238[5]
8420	5.979[4]	7.214[4]	1.962[5]	2.200[5]	2.678[5]	3.389[5]
8421	−8.081[3]	−9.702[3]	−2.625[4]	−2.970[4]	−3.612[4]	−4.566[4]
8422	4.380[2]	5.183[2]	1.380[3]	1.603[3]	1.945[3]	2.453[3]

premise that the molecules are in the rovibrational ground state. As such $\Omega \equiv 0$ and $M = 0$ (the use of a dc external field will not mix different M values), reducing both Eqs. (22) and (24) significantly. In Fig. 3 we have plotted the dc field dressed electrostatic moments as a function of the external field strength. While the very high field strengths in Fig. 3 are generally experimentally challenging, it is illustrative to show how difficult it is to obtain both strong orientation ($\langle\cos\theta\rangle > 0.85$) and alignment ($\langle\cos^2\theta\rangle > 0.85$) in molecules with small rotational constants, regardless of the strength of the dipole moment. It is also instructive to examine the low-field strengths of Fig. 3, where the linear trend of each curve on the log-log scale shows the general scaling of the static moments as a function of the external field as discussed in Sec. IV B. In Fig. 4 we have evaluated Eq. (22) for KRb (KRb is chosen for its medium-strength dipole moment and large rotational constant) at various dc field strengths. This is done by numerically diagonalizing Eq. (5) for each field strength F to obtain Eq. (23), after which Eq. (22) can evaluated for any intermolecular distance **R**. In diagonalizing Eq. (5) a question of the size of the rotational basis set expansion in Eq. (3) arises. Performing a convergence test, it was determined that including between 15 and 30 rotational states in the expansion is sufficient for all the molecules studied. Examining Fig. 4, the difference between the low and high field strengths is easily identified by the change in behavior from most similar to the field-free case (e.g., isotropic contributions dominate the interaction potential) to the regime where the dressed-state van der Waals interaction energy more closely resembles the molecule-fixed-frame van der Waals potential (e.g., when electrostatic contributions become key). This high-field-strength regime is more quantitatively defined when both $\langle\cos\theta\rangle$ and $\langle\cos^2\theta\rangle$ are greater than 0.9 (which corresponds to roughly seven strongly coupled rotational states). Also in Fig. 4 the approximate two-state model of Eq. (29) can be seen to agree very well with the fully coupled equations in the low-field limit. Fully field-coupled potentials for the other heteronuclear molecules

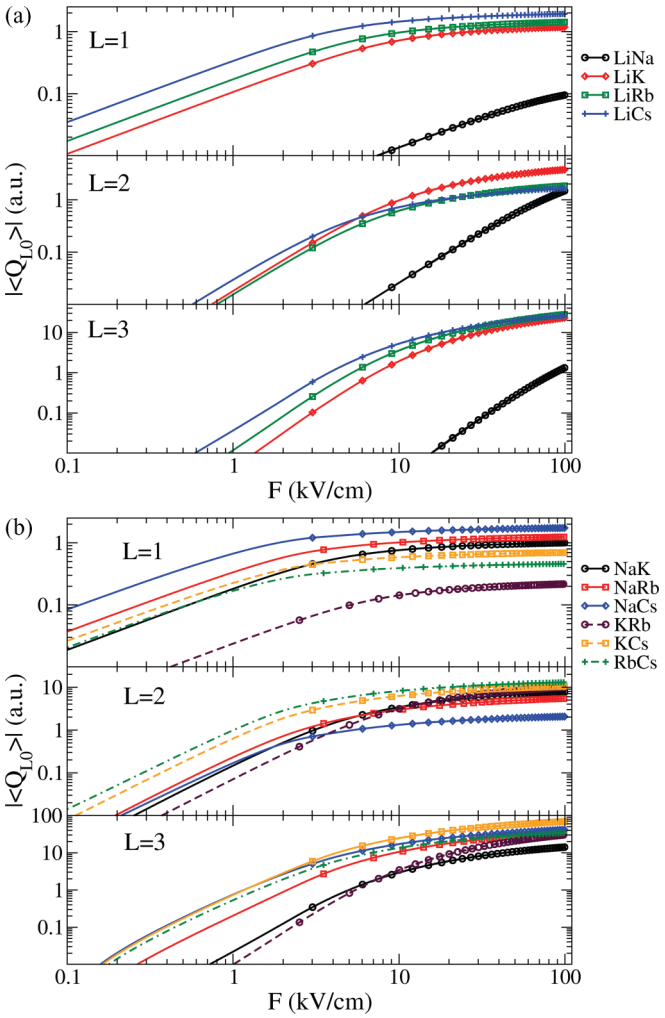

FIG. 3. (Color online) Dressed-state electrostatic moments $\langle Q_{\ell 0}^{DS} \rangle$ ($\ell = 1,2,3$ corresponds to dipole, quadrupole, and octopole moments, respectively) of (a) LiX and (b) NaX, KX, and RbCs (X = Na, K, Rb, Cs as appropriate) as a function of an external dc electric field.

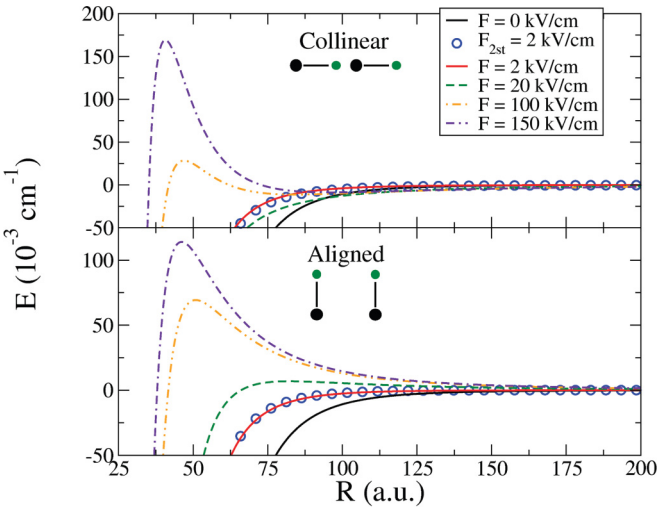

FIG. 4. (Color online) The dc field-coupled van der Waals curves [Eq. (22) with $M_i = M_i' = 0$] of ^{40}K^{87}Rb for both low and high fields as well as the approximate two-state van der Waals curve [Eq. (29)]. Here $F \sim 20$ kV/cm is the intermediate field strength where more than two rotational states begin to strongly couple.

listed in this work have been calculated and are available upon request.

VII. CONCLUSIONS

This work completes our systematic TD-DFT computation of the alkali-metal diatomic species by computing accurate multipole electrostatic moments and anisotropic van der Waals coefficients for the heteronuclear alkali-metal diatomic species. The multipole electrostatic moments were computed using a finite-field treatment of the CCSD(T) molecular energy employing the augmented Karlsruhe def2-QZVPP basis set and were found to produce excellent agreement with the existing literature. Excitation energies and multipole transition moments were calculated using TD-DFT and the same augmented QZVPP basis set. Static polarizabilities as well as van der Waals induction and dispersion coefficients were evaluated using the sum-over-states approach and were found to be consistent with the existing literature. Using the simple form of Eq. (9) and the values from Tables IV and V, it is possible to completely characterize the long-range interaction between two heteronuclear alkali-metal diatoms up through order R^{-8}. A sample FORTRAN program for evaluating Eq. (9) is included in the supplemental material of Ref. [31] or upon request to the authors.

The transformation of the van der Waals series for linear molecules from the molecule-fixed frame to the laboratory-fixed frame was described. This was followed by the computation of the dressed-state electrostatic moments as a function of an external dc electric field. It was noted that in the low-field limit the coupling of the molecule to the external field can be approximated by only considering two rotational states. With this in mind, the orientation and alignment of the molecule as a function of the applied field can be approximated using only molecular spectroscopic constants by Eqs. (25)–(28), which are valid for field values $F \leqslant 2B/\mathcal{D}$. We have also illustrated the effects of an external dc electric field on the intermolecular potential by evaluating Eq. (22) for ^{40}K^{87}Rb at a variety of field strengths. It can be seen then that introducing rotational state coupling leads to a richer interaction phase space beyond the usual isotropic approximations. Finally, a two-state approximation of the dressed-state long-range potential [see Eq. (22)] has been derived and is given by Eq. (29) in terms of molecular spectroscopic constants and isotropic van der Waals coefficients

ACKNOWLEDGMENTS

J.B. would like to thank the Department of Defense Air Force Office of Scientific Research MURI grant for support, and R.C. would like to thank the Chemical Science, Geoscience and Bioscience Division of the Office of Basic Energy Science, Office of Science, US Department of Energy.

[1] M. de Miranda, A. Chotia, B. Neyenhuis, D. Wang, G. Quéméner, S. Ospelkaus, J. Bohn, J. Ye, and D. Jin, Nat. Phys. **7**, 502 (2011).

[2] J. Deiglmayr, M. Repp, R. Wester, O. Dulieu, and M. Weidemüller, Phys. Chem. Chem. Phys. **13**, 19101 (2011).

[3] D. DeMille, F. Bay, S. Bickman, D. Kawall, D. Krause, S. E. Maxwell, and L. R. Hunter, Phys. Rev. A **61**, 052507 (2000).

[4] D. DeMille, S. Sainis, J. Sage, T. Bergeman, S. Kotochigova, and E. Tiesinga, Phys. Rev. Lett. **100**, 043202 (2008).

[5] N. Balakrishnan and A. Dalgarno, Chem. Phys. Lett. **341**, 652 (2001).

[6] G. Quéméner, N. Balakrishnan, and A. Dalgarno, in *Cold Molecules, Theory, Experiment and Applications*, edited by R. V. Krems, W. C. Stwalley, and B. Friedrich (CRC Press, Boca Raton, FL, 2009), p. 69.

[7] K. Ni, S. Ospelkaus, D. Wang, G. Quéméner, B. Neyenhuis, M. Miranda, J. Bohn, J. Ye, and D. Jin, Nature (London) **464**, 1324 (2010).

[8] G. Quéméner, J. L. Bohn, A. Petrov, and S. Kotochigova, Phys. Rev. A **84**, 062703 (2011).

[9] R. V. Krems, Phys. Chem. Chem. Phys. **10**, 4079 (2008).

[10] A. Micheli, G. K. Brennen, and P. Zoller, Nat. Phys. **2**, 341 (2006).

[11] L. Santos, G. V. Shlyapnikov, P. Zoller, and M. Lewenstein, Phys. Rev. Lett. **85**, 1791 (2000).

[12] A. Recati, P. O. Fedichev, W. Zwerger, and P. Zoller, Phys. Rev. Lett. **90**, 020401 (2003).

[13] S. F. Yelin, K. Kirby, and R. Côté, Phys. Rev. A **74**, 050301(R) (2006).

[14] S. F. Yelin, D. DeMille, and R. Côté, in *Cold Molecules, Theory, Experiment and Applications*, edited by R. V. Krems, W. C. Stwalley, and B. Friedrich (CRC Press, Boca Raton, FL, 2009), p. 629.

[15] E. Kuznetsova, M. Gacesa, S. F. Yelin, and R. Côté, Phys. Rev. A **81**, 030301 (2010).

[16] B. Segev, R. Côté, and M. G. Raizen, Phys. Rev. A **56**, R3350 (1997).

[17] S. Kallush, B. Segev, and R. Côté, Phys. Rev. Lett. **95**, 163005 (2005).

[18] K. Shimshon, B. Segev, and R. Côté, Eur. Phys. J. D. **35**, 3 (2005).

[19] L. Holmegaard, J. H. Nielsen, I. Nevo, H. Stapelfeldt, F. Filsinger, J. Kupper, and G. Meijer, Phys. Rev. Lett. **102**, 023001 (2009).

[20] J. H. Nielsen, H. Stapelfeldt, J. Küpper, B. Friedrich, J. Omiste, and R. González-Férez, Phys. Rev. Lett. **108**, 193001 (2012).

[21] J. N. Byrd, J. A. Montgomery, Jr., and R. Côté, Phys. Rev. A **82**, 010502(R) (2010).

[22] P. S. Żuchowski and J. M. Hutson, Phys. Rev. A **81**, 060703 (2010).

[23] J. N. Byrd, H. H. Michels, J. A. Montgomery, Jr., R. Côté, and W. C. Stwalley, J. Chem. Phys. **136**, 014306 (2012).

[24] Q. Wei, S. Kais, B. Friedrich, and D. Herschbach, J. Chem. Phys. **134**, 124107 (2011).

[25] P. F. Weck and N. Balakrishnan, Int. Rev. Phys. Chem. **25**, 283 (2006).

[26] A. D. Buckingham, Adv. Chem. Phys. **12**, 107 (1967).

[27] W. T. Zemke, J. N. Byrd, H. H. Michels, J. A. Montgomery, Jr., and W. C. Stwalley, J. Chem. Phys. **132**, 244305 (2010).

[28] A. Banerjee, A. Chakrabarti, and T. K. Ghanty, J. Chem. Phys. **127**, 134103 (2007).

[29] A. Banerjee, A. Chakrabarti, and T. K. Ghanty, Int. J. Quantum Chem. **109**, 1376 (2009).

[30] D. Spelsberg, T. Lorenz, and W. Meyer, J. Chem. Phys. **99**, 7845 (1993).

[31] J. N. Byrd, R. Côté, and J. A. Montgomery, Jr., J. Chem. Phys. **135**, 244307 (2011).

[32] S. Kotochigova, New J. Phys. **12**, 073041 (2010).

[33] J. Deiglmayr, A. Grochola, M. Repp, K. Mörtlbauer, C. Glück, J. Lange, O. Dulieu, R. Wester, and M. Weidemüller, Phys. Rev. Lett. **101**, 133004 (2008).

[34] M. Aymar and O. Dulieu, J. Chem. Phys. **122**, 204302 (2005).

[35] S. Kotochigova, P. S. Julienne, and E. Tiesinga, Phys. Rev. A **68**, 022501 (2003).

[36] K. Tang, Phys. Rev. **177**, 108 (1969).

[37] The orientation and alignment of a dipole in an external field is given by the dipole-vector and field-vector correlation distribution. Expanding the distribution in terms of Legendre polynomials, the first odd term is $\cos\theta$, corresponding to the *orientation cosine*, and the first even term is $\cos^2\theta$, corresponding to the *alignment cosine*.

[38] A. R. Edmonds, Angular Momentum in Quantum Mechanics (Princeton University Press, Princeton, NJ, 1960).

[39] M. Härtelt and B. Friedrich, J. Chem. Phys. **128**, 224313 (2008).

[40] F. Mulder, A. van der Avoird, and P. E. S. Wormer, Mol. Phys. **37**, 159 (1979).

[41] A. van der Avoird, P. E. S. Wormer, F. Mulder, and R. M. Berns, Top. Curr. Chem. **93**, 1 (1980).

[42] In principle the summation over k_i in Eqs. (12) and (13) involves an integral-sum over continuum states. In practice we truncate the summation to include all single excitations within the electronic Hilbert space.

[43] T. V. Tscherbul, Y. V. Suleimanov, V. Aquilanti, and R. V. Krems, New J. Phys. **11**, 055021 (2009).

[44] M. Urban and A. J. Sadlej, J. Chem. Phys. **103**, 9692 (1995).

[45] N. P. Labello, A. M. Ferreira, and H. A. Kurtz, J. Comput. Chem. **26**, 1464 (2005).

[46] N. P. Labello, A. M. Ferreira, and H. A. Kurtz, Int. J. Quantum. Chem. **106**, 3140 (2006).

[47] J. Harrison and D. Lawson, Int. J. Quantum Chem. **102**, 1087 (2005).

[48] F. Weigend, F. Furche, and R. Ahlrichs, J. Chem. Phys. **119**, 12753 (2003).

[49] Y. Tawada, T. Tsuneda, S. Yanagisawa, Y. Yanai, and K. Hirao, J. Chem. Phys. **120**, 8425 (2004).

[50] A. Dreuw and M. Head-Gordon, Chem. Rev. **105**, 4009 (2005).

[51] K. Raghavachari, G. W. Trucks, J. A. Pople, and M. Head-Gordon, Chem. Phys. Lett. **157**, 479 (1989).

[52] M. W. Schmidt, K. K. Baldridge, J. A. Boatz, S. T. Elbert, M. S. Gordon, J. J. Jensen, S. Koseki, N. Matsunaga, K. A. Nguyen, S. Su, T. L. Windus, M. Dupuis, and J. A. Montgomery, Jr., J. Comput. Chem. **14**, 1347 (1993).

[53] M. S. Gordon and M. W. Schmidt, in *Theory and Applications of Computational Chemistry, the First Forty Years*, edited by C. E. Dykstra, G. Frenking, K. S. Kim, and G. E. Scuseria (Elsevier, Amsterdam, 2005), p. 1167.

[54] H.-J. Werner *et al.*, MOLPRO, version 2010.1, a package of *ab initio*programs, 2010; see http://www.molpro.net.

[55] P. Julienne, T. Hanna, and Z. Idziaszek, Phys. Chem. Chem. Phys. **13**, 19114 (2011).

[56] J. N. Byrd, J. A. Montgomery, Jr., and R. Côté, Phys. Rev. Lett. **109**, 083003 (2012).

[57] It should be reiterated that from an alignment point of view, obtaining field-dressed electrostatic moments sizable enough to produce long-range barriers requires electric field strengths that are experimentally intractable ($F \gtrsim 30$ kV/cm). However, from a molecule-fixed-frame collision point of view the merits of including these electrostatic moments is then independent of the external field strength, and Eq. (33) should then be referenced.

[58] R. González-Férez, M. Mayle, P. Sãnchez Moreno, and P. Schmelcher, Europhys. Lett. **83**, 43001 (2008).

[59] P. Calaminici, K. Jug, and A. Köster, J. Chem. Phys. **109**, 7756 (1998).

[60] C. Adamo, M. Cossi, G. Scalmani, and V. Barone, Chem. Phys. Lett. **307**, 265 (1999).

[61] T. B. Adler, G. Knizia, and H.-J. Werner, J. Chem. Phys. **127**, 221106 (2007).

[62] G. Knizia, T. B. Adler, and H.-J. Werner, J. Chem. Phys. **130**, 054104 (2009).

[63] Even at the highly correlated level of theory used in computing the *ab initio* curves in Fig. 2, there is a several cm $^{-1}$ difference in barrier heights between the F12a and F12b explicitly correlated methods, demonstrating the difficulty in obtaining reliable results for molecular interaction barriers at long range.